DYNAMIC RESPONSE ANALYSIS OF PYLON RELEASE FOR FLEXIBLE AIRCRAFTS

Chen Song, Changchuan Xie* and Yali Shao

*School of Aeronautic Science and Engineering
Beihang University,
Xueyuan Road 37, 100191 Beijing

China

ABSTRACT

Surveillance and strike UAVs, such as the U.S. MQ-9 Reaper and Chinese Wing Loong-2, are pivotal in modern warfare, valued for their long endurance and precision strike capability. To balance performance, most adopt high-aspect-ratio wings, which exhibit significant flexibility due to lightweight design; under loads or mass changes, they undergo notable elastic deformation, leading to rigid-elastic coupling as structural modal frequencies approach rigid-body motion frequencies. Pylon release imposes multiple disturbances on these UAVs, including mass variation, transient recoil, and deformation-induced aerodynamic changes, yet rigid-body models ignore such coupling, resulting in inaccurate safety evaluations. While mainstream CFD-CSD coupling methods ensure accuracy, their inefficiency—stemming from dynamic meshing and small time steps—fails to meet engineering demands for rapid release process simulation.

In this paper, the flight dynamics equations of flexible aircraft are established under the mean axis coordinate system, where modal truncation is used for structural dynamics, and the elastic coupled formula can be simplified as follows:

$$\begin{cases} \dot{\boldsymbol{V}} = -\tilde{\boldsymbol{\omega}}\boldsymbol{V} + \boldsymbol{\Phi}_{\mathrm{t}}^{\mathrm{T}}\left(\boldsymbol{f}_{\mathrm{G}} + \boldsymbol{f}_{\mathrm{A}} + \boldsymbol{f}_{\mathrm{T}}\right)/M \\ \dot{\boldsymbol{\omega}} = -\boldsymbol{J}^{-1}\tilde{\boldsymbol{\omega}}\boldsymbol{J}\boldsymbol{\omega} + \boldsymbol{J}^{-1}\boldsymbol{\Phi}_{\mathrm{r}}^{\mathrm{T}}\left(\boldsymbol{f}_{\mathrm{G}} + \boldsymbol{f}_{\mathrm{A}} + \boldsymbol{f}_{\mathrm{T}}\right) \\ \boldsymbol{M}_e\ddot{\boldsymbol{q}}_e + \boldsymbol{B}_e\dot{\boldsymbol{q}}_e + \boldsymbol{K}_e\boldsymbol{q}_e = \boldsymbol{\Phi}_e^{\mathrm{T}}\left(\boldsymbol{f}_{\mathrm{G}} + \boldsymbol{f}_{\mathrm{A}} + \boldsymbol{f}_{\mathrm{T}}\right) \\ \dot{\boldsymbol{R}}_g = \boldsymbol{L}^{\mathrm{T}}\boldsymbol{V} \\ \dot{\boldsymbol{\Theta}} = \boldsymbol{D}^{-1}\boldsymbol{\omega} \end{cases} \tag{1}$$

where $\boldsymbol{\Phi}_t, \boldsymbol{\Phi}_r, \boldsymbol{\Phi}_e$ denotes the translational, rotational, and elastic modes respectively; $\boldsymbol{f}_{\mathrm{G}}, \boldsymbol{f}_{\mathrm{A}}$, $\boldsymbol{f}_{\mathrm{T}}$ is the node load caused by gravity, aerodynamic force, and propulsion respectively.

The aerodynamic load is computed via the unsteady vortex lattice method (UVLM). In the classic method, the strengths of the bound vortices $\boldsymbol{\Gamma}_b$ and trailing vortices $\boldsymbol{\Gamma}_w$ are updated in a time-marching manner. This study derives a mathematically equivalent continuous-time state update equation:

$$\dot{\boldsymbol{\Gamma}}_w(t) = \boldsymbol{A}_c\boldsymbol{\Gamma}_w(t) + \boldsymbol{B}_c\boldsymbol{w}(t) \tag{2}$$

where $\boldsymbol{w}$ denotes the normal downwash at the collocation points, comprising the normal components of the free-stream and wing elastic vibration velocity. $\boldsymbol{A}_c$ and $\boldsymbol{B}_c$ are coefficient matrixes determined by the mesh discretization and free-stream parameters. By performing eigenvalue decompositon on matrix $\boldsymbol{A}_c$, the aerodynamic order reduction can be achieved via modal truncation, and the aerodynamic generalized coordinates are denoted as $\boldsymbol{q}_a$.

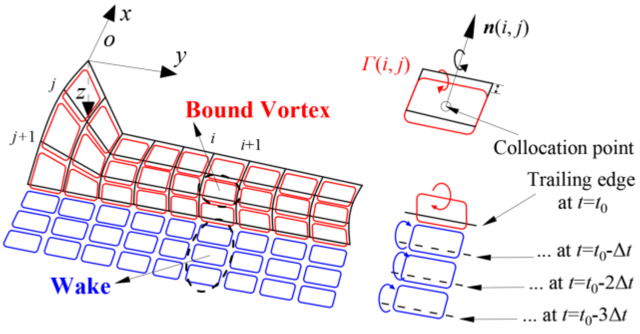

Figure 1: Schematic diagram of classic UVLM

By choosing $\boldsymbol{x}=[\Delta\dot{\boldsymbol{V}} \quad \Delta\dot{\boldsymbol{\theta}} \quad \Delta\dot{\boldsymbol{\omega}} \quad \dot{\boldsymbol{q}}_a \quad \dot{\boldsymbol{q}}_e \quad \ddot{\boldsymbol{q}}_e]^T$ as state-variable and $\boldsymbol{u}=[\boldsymbol{\delta} \quad \dot{\boldsymbol{\delta}} \quad \boldsymbol{f}_{dir}]$ as input variable, the small-disturbance equation in the state-space form can be obtained as follows:

$$\dot{\boldsymbol{x}}=\boldsymbol{A}\boldsymbol{x}+\boldsymbol{B}\boldsymbol{u} \tag{3}$$

where $\boldsymbol{\delta}$ denotes the control surface deflection, $\boldsymbol{f}_{dir}$ denotes direct force input, such as the impact load during pylon release.

To calculate the aircraft's dynamic response of pylon release, it is first necessary to compute the steady-level trim values before and after weapon release, denoted as $\bar{\boldsymbol{x}}_1$ and $\bar{\boldsymbol{x}}_2$ respectively. Assuming the aircraft is steady before weapon release and set the release instant as the initial simulation time, the dynamic response of flexible aircraft would be calculated using the small-disturbance equation established with after-release structural properties, where the initial condition is $\boldsymbol{x}_0=\bar{\boldsymbol{x}}_1-\bar{\boldsymbol{x}}_2$.

A high-aspect-ratio UAV model is adopted as the numerical example, with a 50-kg payload mounted on each wing at the position 1/3 of the wingspan from the wing root.

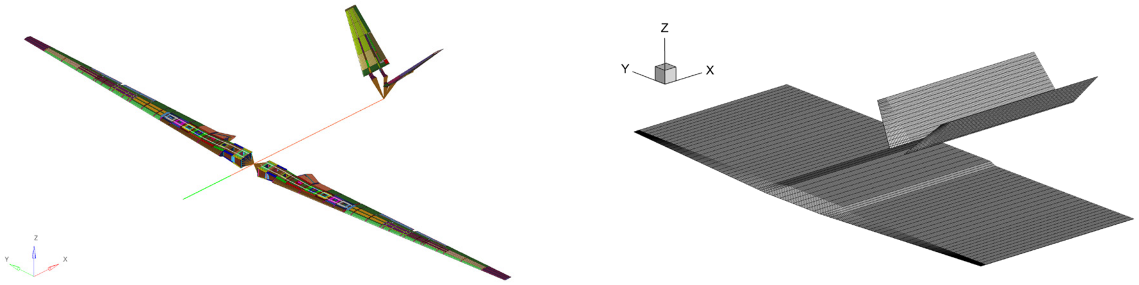

(a) FEM model

(b) UVLM model with wake zone

Figure 2: Modeling of the numerical example

Taking the release of the left-side payload as an example, the steady-level flight states are first calculated for two cases: payload mounted on both wings and payload mounted only on the right side.

Table 1: Trim states before and after left payload release

trim state	payload on both sides	payload only on right side
angle of attack	2.10°	1.98°

left aileron deflection	0.01°	-0.70°
right aileron deflection	-0.01°	0.70°
left V-tail deflection	-5.03°	-4.81°
right V-tail deflection	-5.05°	-4.85°
left wingtip elastic deformation	141.62mm	130.76mm
right wingtip elastic deformation	141.67mm	141.23mm

A half-cycle sin function is employed to simulate the ejection impact during pylon release. The dynamic response calculated using the proposed elastic coupled formula and the traditional rigid-body flight dynamics are presented as follows.

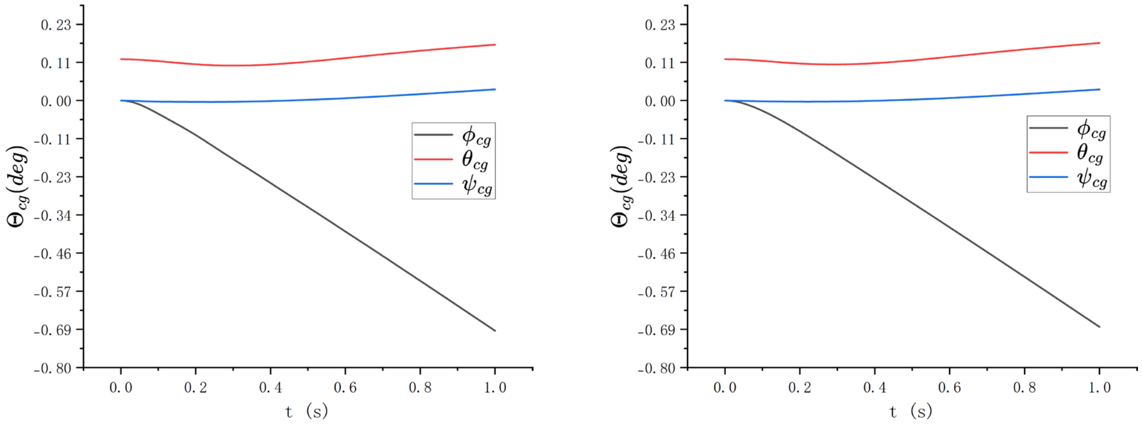

(a.1) attitude response for flexible aircraft (a.2) attitude response for rigid aircraft

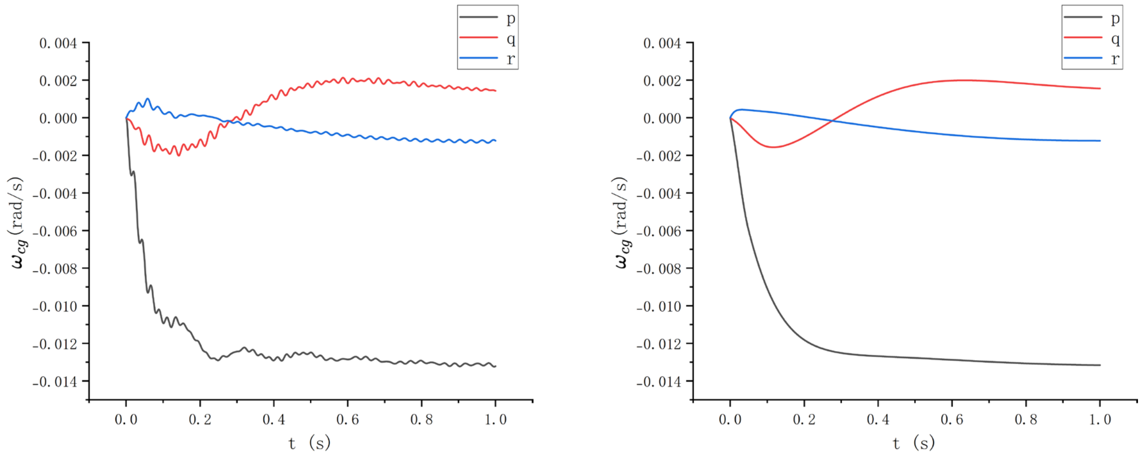

(b.1) angular velocity response for flexible aircraft (b.2) angular velocity response for rigid aircraft

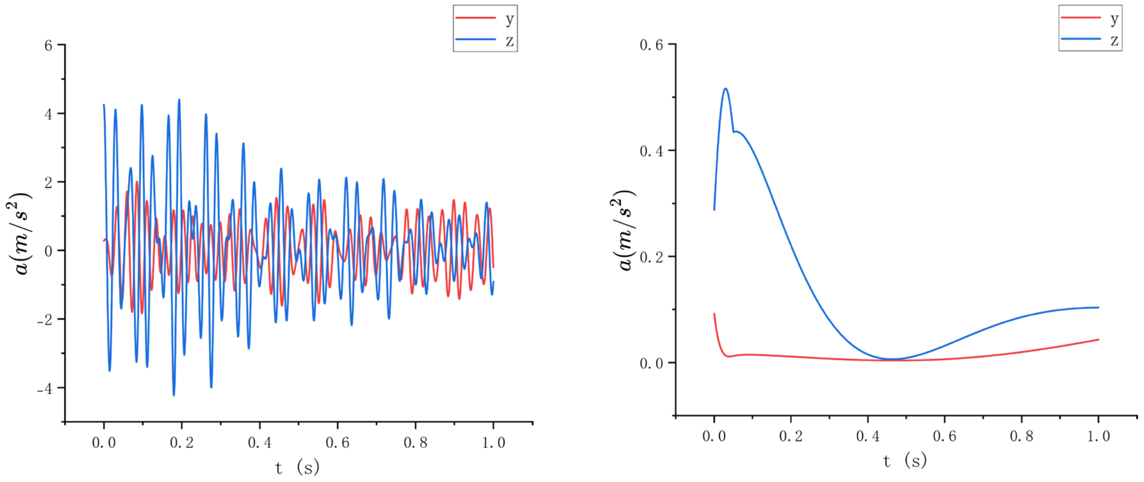

(c.1) acceleration response at centre of mass for flexible aircraft

(c.2) acceleration response at centre of mass for rigid aircraft

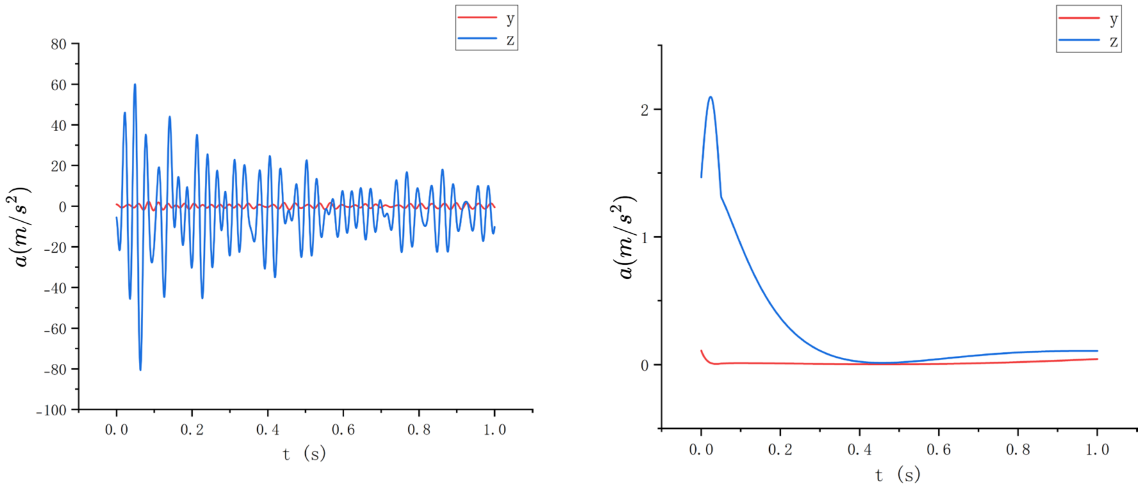

(d.1) acceleration response at left wingtip for flexible aircraft

(d.2) acceleration response at left wingtip for rigid aircraft

Figure 3: Dynamic response calculated using the proposed elastic coupled formula and the traditional rigid-body flight dynamics

In conclusion, this study investigates the dynamic response of aircraft during pylon release, revealing that the combined effects of sudden mass change and ejection impact load induce significant overload, angular velocity fluctuations at the centre of mass, and pronounced wing elastic vibrations. Compared with the classic rigid-body flight dynamics model, which simplifies physical processes and underestimates response complexity and peak loads, the proposed method more accurately captures the aeroelasticity-flight dynamics coupling mechanism, highlighting the non-negligible influence of structural flexibility on the transient response. This finding emphasizes that structural flexibility must be prioritized in the design of high-aspect-ratio aircraft, providing valuable insights for dynamic analysis and design optimization of flexible aircraft under transient loads like pylon release.